Autophagy Competes for a Common Phosphatidylethanolamine Pool with Major Cellular PE-Consuming Pathways in *Saccharomyces cerevisiae*

Caroline Wilson-Zbinden,* Aline Xavier da Silveira dos Santos,† Ingrid Stoffel-Studer,* Aniek van der Vaart,‡ Kay Hofmann,§ Fulvio Reggiori,‡ Howard Riezman,† Claudine Kraft,*, and Matthias Peter*,[1]**

*Department of Biology, Institute of Biochemistry, ETH Zurich, 8093 Zürich, Switzerland, †Department of Biochemistry, University of Geneva, 1211 Geneva 4, Switzerland, ‡Department of Cell Biology, Center for Molecular Medicine, University Medical Center Utrecht, Heidelberglaan 100, 3584 CX Utrecht, The Netherlands, §Institute for Genetics, University of Cologne, Zülpicherstrasse 47a, D-50674 Cologne, Germany, and **Department for Biochemistry and Cell Biology, Max F. Perutz Laboratories, University of Vienna, A-1030 Vienna, Austria

ABSTRACT Autophagy is a highly regulated pathway that selectively degrades cellular constituents such as protein aggregates and excessive or damaged organelles. This transport route is characterized by engulfment of the targeted cargo by autophagosomes. The formation of these double-membrane vesicles requires the covalent conjugation of the ubiquitin-like protein Atg8 to phosphatidylethanolamine (PE). However, the origin of PE and the regulation of lipid flux required for autophagy remain poorly understood. Using a genetic screen, we found that the temperature-sensitive growth and intracellular membrane organization defects of *mcd4-174* and *mcd4-P301L* mutants are suppressed by deletion of essential autophagy genes such as *ATG1* or *ATG7*. *MCD4* encodes an ethanolamine phosphate transferase that uses PE as a precursor for an essential step in the synthesis of the glycosylphosphatidylinositol (GPI) anchor used to link a subset of plasma membrane proteins to lipid bilayers. Similar to the deletion of *CHO2*, a gene encoding the enzyme converting PE to phosphatidylcholine (PC), deletion of *ATG7* was able to restore lipidation and plasma membrane localization of the GPI-anchored protein Gas1 and normal organization of intracellular membranes. Conversely, overexpression of Cho2 was lethal in *mcd4-174* cells grown at restrictive temperature. Quantitative lipid analysis revealed that PE levels are substantially reduced in the *mcd4-174* mutant but can be restored by deletion of *ATG7* or *CHO2*. Taken together, these data suggest that autophagy competes for a common PE pool with major cellular PE-consuming pathways such as the GPI anchor and PC synthesis, highlighting the possible interplay between these pathways and the existence of signals that may coordinate PE flux.

KEYWORDS autophagy; Atg8; phospholipids; GPI anchor; Mcd4

LOCAL glycerophospholipid levels depend on several processes, including biosynthesis, remodeling, degradation, and interorganellar trafficking. Phosphatidylethanolamine (PE) and phosphatidylcholine (PC) are key building blocks of membrane bilayers and account for up to 50% of phospholipids in eukaryotic cells. PE is typically synthesized from phosphatidylserine (PS) by phosphatidylserine decarboxylases (Psd1 and Psd2) and can be converted to PC through the addition of three methyl groups by the methyltransferases Cho2 and Opi3 (Mcgraw and Henry 1989). Cho2 is required for the first methylation reaction during PC biosynthesis, and Opi3 catalyzes the last two steps (Carman and Han 2011). PE also can be generated through the Kennedy (or salvage) pathway from diacylglycerol and ethanolamine by the sequential action of Eki1, Ect1, and Ept1 (Henry *et al.* 2012; McMaster and Bell 1994). In addition to serving as main constituents of membrane bilayers, PE is also used to covalently modify a subset of proteins, thereby regulating several cellular pathways, including glycosylphosphatidylinositol (GPI) anchoring and autophagy. However, little is known about how eukaryotic cells coordinate PE homeostasis and distribution into these different pathways.

doi: 10.1534/genetics.114.169797
Manuscript received August 15, 2014; accepted for publication December 5, 2014; published Early Online December 17, 2014.
Supporting information is available online at http://www.genetics.org/lookup/suppl/doi:10.1534/genetics.114.169797/-/DC1
[1]Corresponding author: Institute of Biochemistry, ETH Zurich, 8093 Zürich, Switzerland. E-mail: matthias.peter@bc.biol.ethz.ch

Autophagy targets subcellular organelles and macromolecular complexes for degradation in vacuoles/lysosomes. This highly conserved process ensures cellular homeostasis and plays crucial roles during nutrient starvation and cellular responses to stress conditions, including pathogen invasion. Autophagosomes are able to sequester portions of cytoplasm or specific cargo and rapidly deliver them into the lysosomes/vacuoles for degradation (Suzuki *et al.* 2002). Yeast cells also use the related cytoplasm-to-vacuole targeting (Cvt) pathway to selectively deliver specific vacuolar enzymes such as aminopeptidase 1 (Ape1) and α-mannosidase (Ams1) (Harding *et al.* 1995; Hutchins and Klionsky 2001; Yuga *et al.* 2011).

Genetic analyses in yeast have identified over 36 mostly conserved components required for different steps of autophagy, named Atg1 to Atg36 (Suzuki *et al.* 2007; Motley *et al.* 2012). Autophagy activation triggers the formation of the Atg5-Atg12-Atg16 complex, which, in turn, catalyzes the covalent conjugation of the C-terminus of the ubiquitin-like protein Atg8 (LC3, GABARAP, and GABARAP-like proteins in mammals) to PE (Xin *et al.* 2001; He *et al.* 2003). This lipid anchor mediates association of Atg8 with autophagosomal membranes, where it forms a protein coat and binds specific cargo receptors (Behrends *et al.* 2010; Noda *et al.* 2010; Suzuki *et al.* 2010). The amount of Atg8-PE correlates with the size of autophagosomes, suggesting that expression and modification of Atg8 provides a rate-limiting step for flux through the autophagy pathway (Xie *et al.* 2008).

In addition to modifying Atg8, PE serves as a donor molecule at multiple steps in GPI anchor synthesis. These unique glycolipids are generated by the sequential addition of one *N*-acetylglucosamine and three mannose residues on a phosphatidylinositol (PI) molecule. This basic structure is further modified by deacetylation of the *N*-acetylglucosamine and addition of phosphoethanolamine (P-EtN) groups and in most cases additional mannoses. The terminal P-EtN residue is used to covalently link the C-terminus of specific proteins to the GPI anchor through a phosphodiester bond, resulting in protein association with membranes (Canivenc-Gansel *et al.* 1998). In yeast, the GPI biosynthetic pathway is essential for cell growth and survival and targets approximately 60 proteins mostly required for enzymatic functions in cell wall biosynthesis. The synthesis and conjugation of the GPI anchors to target proteins involves at least 19 proteins, named Gpi1 to Gpi19, that are localized to the endoplasmic reticulum (ER). *MCD4* is required to add a P-EtN group to one of the mannose residues composing the GPI anchor sugar core, and a reduction of its activity leads to accumulation of unanchored GPI proteins in the ER. Likewise, deletion of PIG-N, a mammalian homolog of *MCD4*, reduces surface expression of GPI-anchored proteins and loss of the enzyme activity that adds P-EtN groups to Man1 (Hong *et al.* 1999).

We are interested in the mechanisms that regulate autophagy and aim to identify them through the use of genetic screens. Surprisingly, we found that deletion of autophagy genes rescues the lethality of temperature-sensitive (ts) *mcd4-174* cells, implying a functional link between autophagy and GPI anchor biosynthesis. Subsequent characterization of this genetic interaction revealed that this effect is caused by a limited PE pool that is used for multiple pathways, including PC and GPI anchor synthesis and autophagosome formation.

Materials and Methods

Growth conditions and strain construction

Yeast cells were grown in rich medium (YPD; 1% yeast extract, 2% peptone, 2% glucose) or synthetic dextrose medium (SD; 0.17% yeast nitrogen base, 0.5% ammonium sulfate, 2% glucose, amino acids as required). Nitrogen starvation was induced by growing cells to an optical density (OD_{600}) of 0.5–0.8, washing them once in starvation medium (SD-N; 0.17% yeast nitrogen base without amino acids, 2% glucose), and resuspending them in SD-N for 4 hr. The genotype was as follows: RYY52 (MATα *trp1*, *lys2*, *ura3*, *leu2*, *his3*, *suc2*, *psd1-Δ-1*::TRP1), S288C (*his3Δ1 leu2Δ0 met15Δ0 ura3Δ0*), unless otherwise noted. Haploid deletion strains were obtained after dissecting sporulated heterozygous diploid deletion strains purchased from Euroscarf (Frankfurt, Germany), and the kanamycin-resistant haploids were verified by PCR. The ts strains were obtained from the collection provided by the Boone Laboratory (University of Toronto, Canada). The *mcd4Δ atg7Δ* double mutant was constructed by homologous recombination of the corresponding kanMX deletion cassette into the homologous locus of the gene to be deleted in the heterozygous diploid. The double-deletion heterozygous diploid strain was sporulated and dissected, and the resulting spores were checked for viability and replica plated to determine genotype. All strains and plasmids used in this study can be found in File S1.

Screening procedure and validation of candidates

The kanamycin-resistant ts-strain collection (Li *et al.* 2011) was crossed against a bait haploid deletion strain of *atg1Δ*::*NAT* (*can1*::STE2pr-Sp_*his5 lyp1Δ his3Δ leu2Δ ura3Δ met15Δ*) or wild-type (WT) S288C. Haploid cells were selected with the procedure described previously (Tong *et al.* 2001). After the final selection step, haploid cells were pinned in duplicate and grown at permissive (22°), semipermissive (30°), and restrictive (37°) temperatures. Resulting colony size then was analyzed using the Goldeneye software developed by Dr. Serge Pelet. Candidates that were lethal at restrictive temperature in a WT background but that regained viability after deletion of *ATG1* were classified as negative regulators of autophagy. Candidates that remained viable at semipermissive temperature in a WT background but became nonviable on deletion of *ATG1* were defined as activators of autophagy. Promising candidates were manually recrossed by mating before selecting heterozygous diploid cells on YPD plates containing kanamycin and clonat, followed by sporulation on plates as described previously. Spores were manually dissected 7 days after sporulation, and double mutants were selected by replica plating. Serial dilutions of cells were spotted on YPD (1.5 μl of 1×10^7 to 1×10^3 cells/ml) and

grown for 3 days at permissive (22°) or restrictive (37°) temperature. Colony size and number were compared visually.

Assay for YW3548 sensitivity

Plates containing YPD medium in 2% agar were spread with the indicated amounts of YW3548 (Sutterlin *et al.* 1997) in 200 μl of methanol. Tenfold serial dilutions (5-μl spots containing 10^1–10^5 cells) then were spotted onto the plates. Colony growth was determined visually after 5 days of incubation at 30°.

Ethanolamine growth assay

Yeast cells were grown at permissive temperature (22°) in SD (as described previously) to log phase and diluted in SD with or without the addition of 5 mM ethanolamine. Cells then were grown over a period of 30 hr at restrictive temperature (37°), and cell growth was determined periodically by OD_{600} density.

Western blot and Atg8-PE analysis

Cells were grown to log phase and lysed in 250 μM NaOH and 0.5% 2-mercaptoethanol, followed by trichloroacetic acid (TCA) precipitation of total proteins. For Atg8-PE measurements, cells were grown at 37° to OD_{600} 0.8 in SC medium and then resuspended in SD-N and incubated at 37° for 3 hr. TCA precipitates were washed with acetone and resuspended in sample buffer containing 6 M urea. Total protein extracts were separated by SDS-PAGE and transferred onto nitrocellulose. Membranes were blocked with 5% milk and 1% bovine serum albumin and incubated with appropriate antibodies: rabbit polyclonal antiserum against Gas1 (1:25,000), mouse monoclonal antibody against GFP (1:1000; Roche Diagnostics, Rotkreuz, Switzerland), rabbit peptide antibody against Ape1 (1:1000), rabbit polyclonal antiserum against Atg8 (1:1000), mouse monoclonal antibody against Pgk1 (1:3000; Invitrogen, Carlsbad, CA).

Immunofluorescence of Cwp2-VENUS

Cells were transformed with a plasmid p416-Cwp2-VENUS (Castillon *et al.* 2009). Transformed cells were grown overnight in SD-Ura at 22°. Cells were then diluted into SD without uracil and incubated for 4 hr at 37°. Then 5 μl of cells was spotted onto a microscope slide, and live cells were imaged using a Zeiss Axiovert 200 (Thornwood, NY). Localization of Cwp2-VENUS to the plasma membrane was analyzed visually in >100 cells/strain in three independent experiments.

Electron microscopic analysis of strains

Strains were grown overnight at 22° in YPD, diluted into YPD, and grown at 37° for 3 hr. Electron microscopic (EM) analysis was carried out as described previously (Griffith *et al.* 2008).

Lipid analysis

Cells were grown in rich medium until saturation, diluted to 0.2 OD/ml, and incubated at 22° or 37° for 6 hr. Lipids were quantified as described by Santos *et al.* (2014) (different fonts). Briefly, cells were resuspended in 1.5 ml of extraction solvent [ethanol, water, diethyl ether, pyridine, and 4.2 N ammonium hydroxide (15:15:5:1:0.018 v/v)]. A mixture of internal standards (7.5 nmol 17:0/14:1 PC, 7.5 nmol 17:0/14:1 PE, 6.0 nmol 17:0/14:1 PI, 4.0 nmol 17:0/14:1 PS, 1.2 nmol C17:0-ceramide, and 2.0 nmol C8-glucosylceramide) and 250 μl of glass beads was added, and the sample was vortexed vigorously (Multitube vortexer, Lab-tek International Ltd., Christchurch, New Zealand) at maximum speed for 5 min and incubated at 60° for 20 min. Cell debris was pelleted by centrifugation at 1800 × *g* for 5 min, and the supernatant was collected. The extraction was repeated once, and the supernatants were combined and dried under a stream of nitrogen or under vacuum in a Centrivap (Labconco Corporation, Kansas City, MO). The sample was divided into two equal aliquots. One-half was used for ceramide and sphingolipid analysis, where we performed an extra step to deacylate glycerophospholipids using monomethylamine reagent [methanol, water, *n*-butanol, methylamine solution (4:3:1:5 v/v)](Cheng *et al.* 2001) to reduce ion suppression owing to glycerophospholipids in sphingolipid detection. For desalting, both lipid extracts were resuspended in 300 μl of water-saturated butanol and sonicated for 5 min. Then 150 μl of LC-MS grade water was added, and samples were vortexed and centrifuged at 3200 × *g* for 10 min to induce phase separation. The upper phase was collected. Another 300 μl of water-saturated butanol was added to the lower phase, and the process was repeated twice. The combined upper phases were dried and kept at −80° until analysis. For glycerophospholipid and sphingolipid analysis by electrospray ionization tandem mass spectrometry (ESI-MS/MS), lipid extracts were resuspended in 500 μl of chloroform:methanol (1:1 v/v) and diluted in chloroform:methanol:water (2:7:1 v/v/v) and chloroform:methanol (1:2 v/v) containing 5 mM ammonium acetate for positive and negative modes, respectively. A Triversa Nanomate (Advion, Ithaca, NY) was used to infuse samples with a gas pressure of 30 Psi and a spray voltage of 1.2 kV on a TSQ Vantage (ThermoFisher Scientific, Waltham, MA). The mass spectrometer was operated with a spray voltage of 3.5 kV in positive mode and 3 kV in negative mode. The capillary temperature was set to 190°. Multiple-reaction monitoring mass spectrometry (MRM-MS) was used to identify and quantify lipid species as described previously (Guan *et al.* 2010). Data were converted and quantified relative to standard curves of internal standards, which had been spiked in prior to extraction. The values were normalized owing to variability between replicates. The average of WT triplicates was set to 1, and the mutant data are presented as fold change (mutant/WT). Values are averages ± SD of at least three independent samples. Details on lipid compounds and experimental results of this study are also available on the website lipidomes.org.

Analysis of Cho2 overexpression

pEGH-Gal1/10-Cho2 was obtained from the yeast GST fusion collection (Zhu *et al.* 2001). The plasmid was transformed into cells, and the resulting transformants were analyzed

on plates by sequential dilution spotting onto solid medium containing 2% agar, SC without uracil, and 2% raffinose or 2% galactose. Plates were incubated for 3 days at 22° and 37°.

Results

Identification of novel autophagy regulators among the essential genes

To identify novel regulators of autophagy or essential pathways influenced by autophagy, we screened a large collection of ts mutants in essential genes of *Saccharomyces cerevisiae* for those in which viability is restored by blocking all autophagic processes through deletion of *ATG1* (Figure 1A). The underlying assumption of this approach was that repressors of autophagy might be essential because in their absence this pathway would be constitutively active. Moreover, this genetic screen is expected to identify essential cellular pathways that functionally interact with autophagy. Conversely, positive regulators of autophagy or cellular processes that require an intact autophagy process for viability were screened by isolating ts mutants that are nonviable at nonrestrictive temperature in the absence of *ATG1* (Figure 1A). For both approaches, we deleted *ATG1* by crossing the available ts collection (Li *et al.* 2011) with the *atg1Δ* bait strain (BY7092) and isolated haploid *MAT***a** cells after sporulation and appropriate selection. Synthetic-sick interactions between ts mutants and *atg1Δ* observed at 30° were confirmed by tetrad analysis, and the strength of the genetic interaction was categorized by measuring the colony size of the resulting double mutants (Supporting Information, Table S1A). Interestingly, this analysis identified genes that exhibit synthetic sickness with *atg1Δ* but not with deletions in other autophagy genes, suggesting that Atg1 may have non-autophagy-related functions that will be analyzed in detail elsewhere. The viable *atg1Δ* double mutants were shifted to the restrictive temperature (37°), and the growing colonies were scored after 3 days. Identified mutants were verified by spotting assays followed by manual dissection (Table S1B). Interestingly, one of the identified potential negative regulators of autophagy was *MCD4* (Gaynor *et al.* 1999) because, in contrast to *mcd4-174* strains, *mcd4-174 atg1Δ* double mutants were able to grow at 37° (Figure 1B). This suppression also was observed by deleting *ATG7* (Figure 1B) or *ATG14* (Figure 1C), and as expected, the effect was lost after complementation of the deletions with plasmids expressing WT Mcd4, Atg7, and Atg14, respectively. In contrast, deletion of *ATG21*, a gene required for the selective cytoplasm-to-vacuole targeting (Cvt) pathway (Meiling-Wesse *et al.* 2004), was unable to rescue the lethality of *mcd4-174* at the restrictive temperature (Figure 1D).

To examine whether the observed phenotype was a general feature of cells with perturbed Mcd4 function, we analyzed whether deletion of *ATG7* was able to restore growth of *mcd4Δ* or cells harboring the *mcd4-P301L* allele (Storey *et al.* 2001). Interestingly, *mcd4-P301L atg7Δ* double mutants were able to grow at restrictive temperature (Figure S1A), implying that this genetic suppression is not limited to a single *mcd4* allele. In contrast, tetrad analysis revealed that deletion of *ATG7* was unable to rescue viability of *mcd4Δ* cells (Figure S1B). Likewise, *atg7Δ* cells were sensitive to the Mcd4 inhibitor YW3548 (Sutterlin *et al.* 1997; Hong *et al.* 1999), implying that loss of autophagy does not bypass the need for residual Mcd4 activity (Figure S1C). Taken together, these results suggest that blocking general autophagy function restores growth of cells with reduced but not abolished Mcd4 activity.

Mcd4 has been characterized previously as an essential enzyme for GPI biosynthesis, and *mcd4-174* cells fail to add the GPI anchor to proteins at restrictive temperature (Zhu *et al.* 2006). To examine whether the observed phenotype was specific for *mcd4-174* or for all mutants displaying GPI anchor biosynthesis defects, we crossed *atg1Δ* cells with ts alleles of *GPI2* (*gpi2-1*) and *GPI13* (*gpi13-5*), two genes functioning up- and downstream of Mcd4 in GPI anchor biosynthesis, respectively, and growth of the resulting double mutants was then analyzed at restrictive temperature. As shown in Figure 1E, deletion of *ATG1* was unable to restore the growth of *gpi2-1* or *gpi13-5* cells, implying that the observed suppression is specific for *mcd4-174*.

The mcd4-174 mutant is defective for general autophagy, and deletion of autophagy rescues its GPI-anchoring deficiency

Cells defective for autophagy are sensitive to nutrient starvation. To test whether *MCD4* may be involved in autophagy, we examined *mcd4-174* cells for starvation sensitivity. We observed that *mcd4-174* cells exhibit reduced viability on prolonged nutrient starvation (Figure 2A).

Next, we measured the flux through selective and bulk autophagy pathways in *mcd4-174* cells shifted to restrictive temperature for 4 hr. Vacuolar maturation of the aminopeptidase Ape1 under nutrient-rich conditions was unaffected (Figure 2B), indicating that the selective Cvt pathway does not require Mcd4. Under autophagy-inducing conditions, however, the unprocessed Ape1 levels were slightly increased in the *mcd4-174* mutant compared with the WT control, revealing a partial defect in general autophagy. To assess the progression of autophagy, cleavage of GFP-Atg8 was monitored under starvation conditions (Kim *et al.* 2001) and found to be significantly delayed in *mcd4-174* cells. We could not observe a significant change in the levels of lipidated Atg8 in *mcd4-174* mutants compared with WT controls (Figure S2), indicating that activation of the autophagy pathway is not affected. Together these data suggest that Mcd4 is not a negative regulator of autophagy but rather may promote general autophagy by a direct or indirect mechanism.

To explore a possible link between the function of Mcd4 in autophagy and its known role in GPI anchor biosynthesis, we tested by light microscopy whether the loss of autophagy improves GPI anchor conjugation to proteins and transport

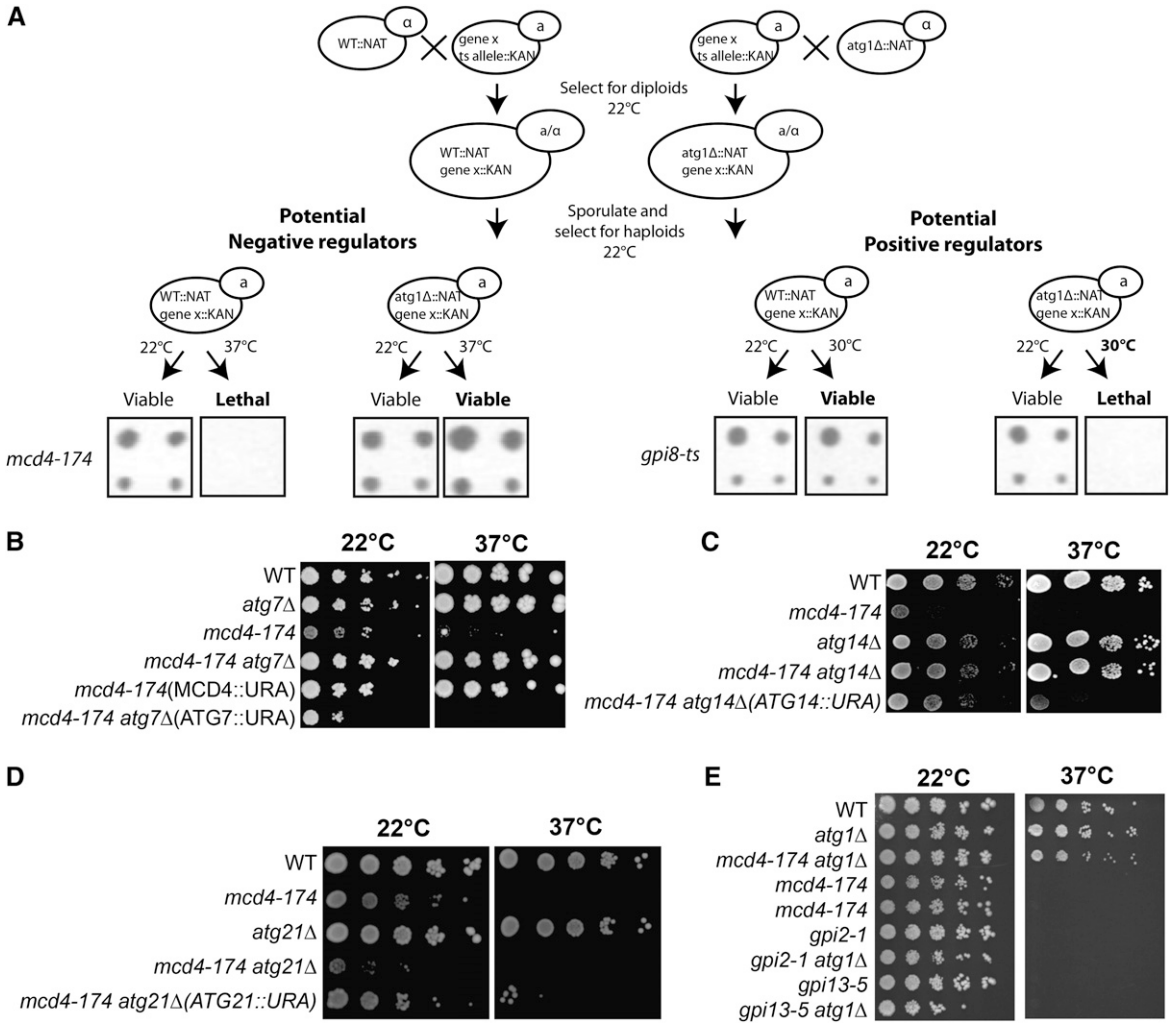

Figure 1 General autophagy mutants can rescue *mcd4-174* lethality. (A) Schematic representation of screening the yeast ts collection for essential genes that are positively or negatively influenced by autophagy. The insets show an example candidate from each, including a member of the GPI-anchoring pathway, *mcd4-174*. (B–D) Dilution spotting of *mcd4-174* crossed with various autophagy mutants. Deletion of genes required for general autophagy is able to rescue the lethality of *mcd4-174* at restrictive temperature. This rescue phenotype was reverted when the WT gene was expressed from a plasmid. Deletion of genes required for specific autophagy pathways, *e.g.*, Cvt (*atg21*), are unable to rescue lethality of *mcd4-174* at restrictive temperature. (E) Dilution spotting of ts alleles of other members of the GPI-anchoring pathway functioning either upstream (Gpi2) or downstream (Gpi13) of Mcd4.

in *mcd4-174* cells. Cell wall protein Cwp2, which undergoes GPI anchoring in the ER before being targeted to the cell wall, was used as a marker. As expected, Cwp2 tagged with the fluorescent VENUS protein localized predominantly to the cell wall of growing buds (scored as normal) but was mostly retained in the ER (scored as abnormal) in the *mcd4-174* strain (Figure 2, C and D). Localization of this fluorescent chimera, however, was almost completely restored in the *mcd4-174 atg7Δ* double mutant but not in the *mcd4-174 atg7Δ* strain reexpressing *ATG7* from a plasmid. GPI anchor linkage to proteins and transport also can be monitored by analyzing the major yeast GPI-anchored protein Gas1 via immunoblotting because the immature ER-resident Gas1 has a molecular weight of 105 kDa compared with 125 kDa for anchored plasma membrane–localized Gas1 (Conzelmann *et al.* 1988). In contrast to WT or *atg7Δ* strains, a faster-migrating unmodified Gas1 species was detectable in *mcd4-174* cells that was absent in the *mcd4-174 atg7Δ* double mutant (Figure 2D). Together these results demonstrate that the *in vivo* function of Mcd4 in GPI anchor biosynthesis is enhanced in the absence of autophagy.

We next examined the morphology of *mcd4-174 atg7Δ* double mutants. In contrast to WT or *atg7Δ* cells, transmission electron microscopic analysis of the *mcd4-174* mutant grown at the restrictive temperature revealed many cellular abnormalities, including the accumulation of abnormal membrane structures, fragmented vacuoles, and cell wall defects (Figure 2, F–I) (Gaynor *et al.* 1999). Strikingly, this phenotype was not observed with the *mcd4-174 atg7Δ* double mutant, suggesting that the cellular phenotypes associated with loss of Mcd4 function are largely suppressed in the absence of autophagy.

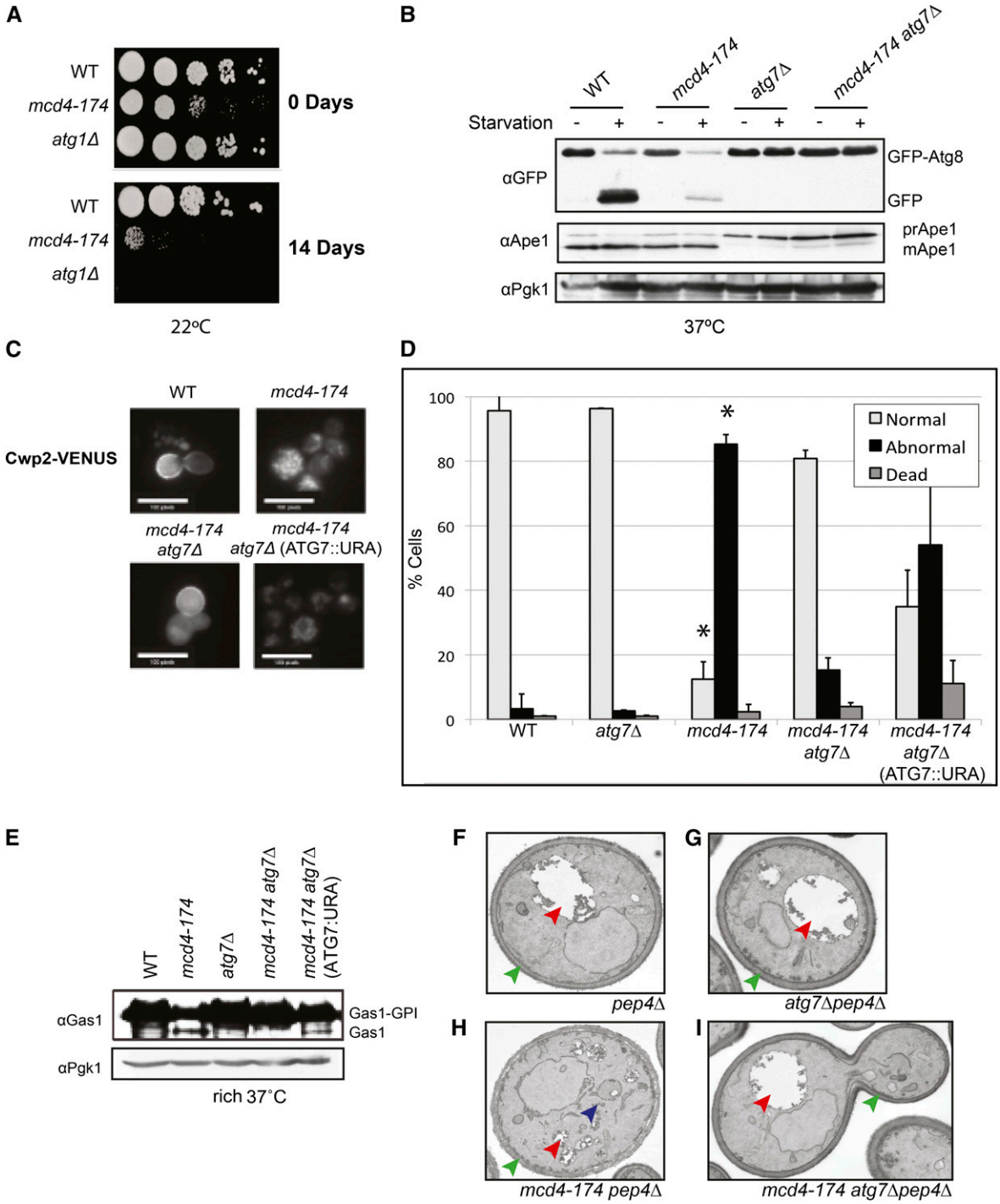

Figure 2 Deletion of the autophagic pathway can rescue defects in GPI anchor synthesis in an *mcd4-174* strain. (A) Dilution spotting of *mcd4-174* cells grown at permissive temperature (22°) under normal nutrient conditions (0 days) or prolonged nutrient starvation (14 days). (B) Western blot analysis of yeast cell lysate derived from WT or mutant cells grown at restrictive temperature (37°, 4 hr) expressing GFP-Atg8. Detection of endogenous Ape1 maturation from its unprocessed precursor (preApe1) to its processed form (mApe1) is used as a readout for the Cvt pathway in rich medium and general autophagy in starvation conditions (see *Materials and Methods*). GFP-Atg8 cleavage is used to monitor general autophagy. Note that *mcd4-174* cells are defective for general autophagy. Detection of endogenous Pgk1p was used as a loading control. (C) The localization of GPI-anchored protein Cwp2-VENUS was analyzed by microscopic analysis in WT and the indicated mutant strains shifted to 37° for 4 hr. Note that Cwp2-VENUS is trapped in the ER in *mcd4-174* mutants, but cell wall localization is restored in *mcd4-174 atg7*Δ cells. (D) Graph of Cwp2-VENUS localization quantification from at least 200 cells with images acquired as in (C) expressed as a percentage of total cells (Normal = cell wall localization; Abnormal = ER localization). Data shown are average and SD of independent biological replicates ($n = 3$). *$P < 0.05$, *t*-test as compared with WT. Note that cell viability is not affected, demonstrating that reduced autophagy in *mcd4-174* cells does not result from excess cell death. (E) Western blot detecting endogenous Gas1 in its GPI-anchored form (Gas1-GPI, higher-MW band) or non-GPI-anchored form (Gas1, lower-MW band) from WT and mutant cell lysates grown in rich medium

Growth of mcd4-174 cells is affected by altering PE levels in vivo by overexpression or deletion of Cho2

Because the GPI anchor biosynthesis and autophagy pathways both require PE as a substrate, we hypothesized that the phenotypes observed in the *mcd4-174* strain could be caused by a reduction in the available PE pool. To test this hypothesis, we genetically altered the cellular PE levels by overexpression or deletion of the PE methyltransferase Cho2, which catalyzes the first step in the conversion of PE to PC (Figure 3, A and B). Indeed, similar to *ATG1* or *ATG7*, deletion of *CHO2* rescued the inviability of *mcd4-174* cells (Figure 3A), and the failure to localize Cwp2-VENUS to the plasma membrane was restored in the *mcd4-174 cho2Δ* double mutants (Figure 3, C and D). Conversely, overexpression of Cho2 from the galactose-inducible *GAL1,10* promoter was lethal in *mcd4-174* but not WT cells grown at 22° on medium containing 2% galactose but not 2% raffinose (Figure 3B). These results support the notion that growth of *mcd4-174* cells might be affected by PE levels because altering the flux of PE-to-PC conversion increases or decreases the viability of the *mcd4-174* cells accordingly.

Loss of autophagy and addition of ethanolamine restores PE levels and proliferation of mcd4-174 cells grown at restrictive temperature

To directly test whether a defect in autophagy also could modulate the cellular PE levels, we compared the lipid composition of WT and different mutant cells at both permissive and restrictive temperatures. While the total amounts of sphingolipids, ceramides, and PI species in all strains were comparable with those in the WT control (Table S2), total PE levels were significantly reduced in *mcd4-174* and surprisingly also in *atg7Δ* cells (Figure 4A). Importantly, however, the PE levels were restored in the *mcd4-174 atg7Δ* and *mcd4-174 cho2Δ* double mutants (Figure 4A), suggesting that increasing PE levels may improve growth of *mcd4-174* cells.

To test this possibility directly, growth of *mcd4-174* cells was measured at restrictive temperature in liquid medium supplemented with ethanolamine, which induces PE synthesis through the Kennedy pathway (Birner *et al.* 2001). While WT and *mcd4-174 atg7Δ* double mutants were unaffected by the addition of ethanolamine, the doubling time of *mcd4-174* cells was significantly increased when grown in the presence of ethanolamine (Figure 4B and data not shown). Together these results suggest that the growth defect of *mcd4-174* cells is manifested, at least in part, from a limited availability of PE for GPI anchor biosynthesis. These results strongly suggest that autophagy inhibition suppresses the growth defect of *mcd4-174* cells by increasing PE levels and thus imply that Mcd4 may play a direct or indirect role in PE metabolism.

To further test this hypothesis, we analyzed the genetic interaction of *mcd4-174* strains with *PSD2*, a gene involved in the conversion of PS to PE in vacuolar membranes, and *ECT1*, a gene of the CDP-ethanolamine pathway. Interestingly, growth of *mcd4-174 psd2Δ* and *mcd4-174 ect1Δ* double mutants at semipermissive temperature (30°) was strongly reduced compared with the corresponding *mcd4-174*, *psd2Δ*, or *ect1Δ* single mutants (Figure S3, A and B). Moreover, *PSD1* and *PSD2* have been shown previously to be effective multicopy suppressors of *fsr2-1* (a mutant allele of *MCD4*) double mutants grown at restrictive temperature (Toh-E and Oguchi 2002). Together these data indicate that the viability of *mcd4-174* cells is affected by generally altering PE levels rather than a specific cellular PE pool.

Discussion

Using a genetic screen, we have identified essential genes that genetically interact with a functional autophagy pathway. Among others, we found that the viability of *mcd4-174* and *mcd4-P301L* cells at restrictive temperature is restored by the deletion of components required for general autophagy. Interestingly, detailed characterization revealed that the amount of PE available for the ethanolamine phosphate transferase Mcd4 becomes limiting under autophagy conditions. Our results thus not only provide new insights into the function of Mcd4 but also help us to understand the flux and regulation of major cellular PE-consuming pathways.

Identification of genetic interacters with genes essential for viability

Systematic screening of the large *S. cerevisiae* collection comprising ts mutants of most essential genes (Li *et al.* 2011) identified a small subset of mutants that positively or negatively depends on a functional autophagy pathway (Table S1). Because autophagy is important for cellular homoeostasis and provides new building blocks by degrading excess or misfolded proteins in the vacuole, synthetic-lethal interactions may reveal components that are involved in quality control or biosynthesis pathways. For example, *SSC1* encodes an ATPase of the Hsp70 chaperon family (Blamowska *et al.* 2010), whereas Nop2 is required for ribosome biogenesis (Hong *et al.* 1997). Conversely, rescue of growth at high temperature identifies deficiencies of essential processes in which autophagy is exacerbating the situation. While the ts mutants in *mcd4-174* and *hyp2-8* were rescued by deleting any essential component of the autophagy pathway, *cmd1-3* and *sec17-1* were suppressed by deleting *ATG1* but not *ATG7*, suggesting that Atg1 may have unknown functions in addition to triggering autophagy (Papinski *et al.* 2014).

at the nonpermissive temperature (37°). In *mcd4-174* but not *mcd4-174 atg7*Δ cells, a lower-MW band accumulates corresponding to nonanchored Gas1. Detection of endogenous Pgk1 was used as a loading control. (F–I) Transmission EM images of mutant yeast cells grown at nonpermissive temperature (37°) showing various GPI-anchoring defects, which are rescued by deletion of the *ATG7* gene required for autophagy (red arrow, vacuole; green arrow, cell wall; blue arrow, accumulation of abnormal membranes).

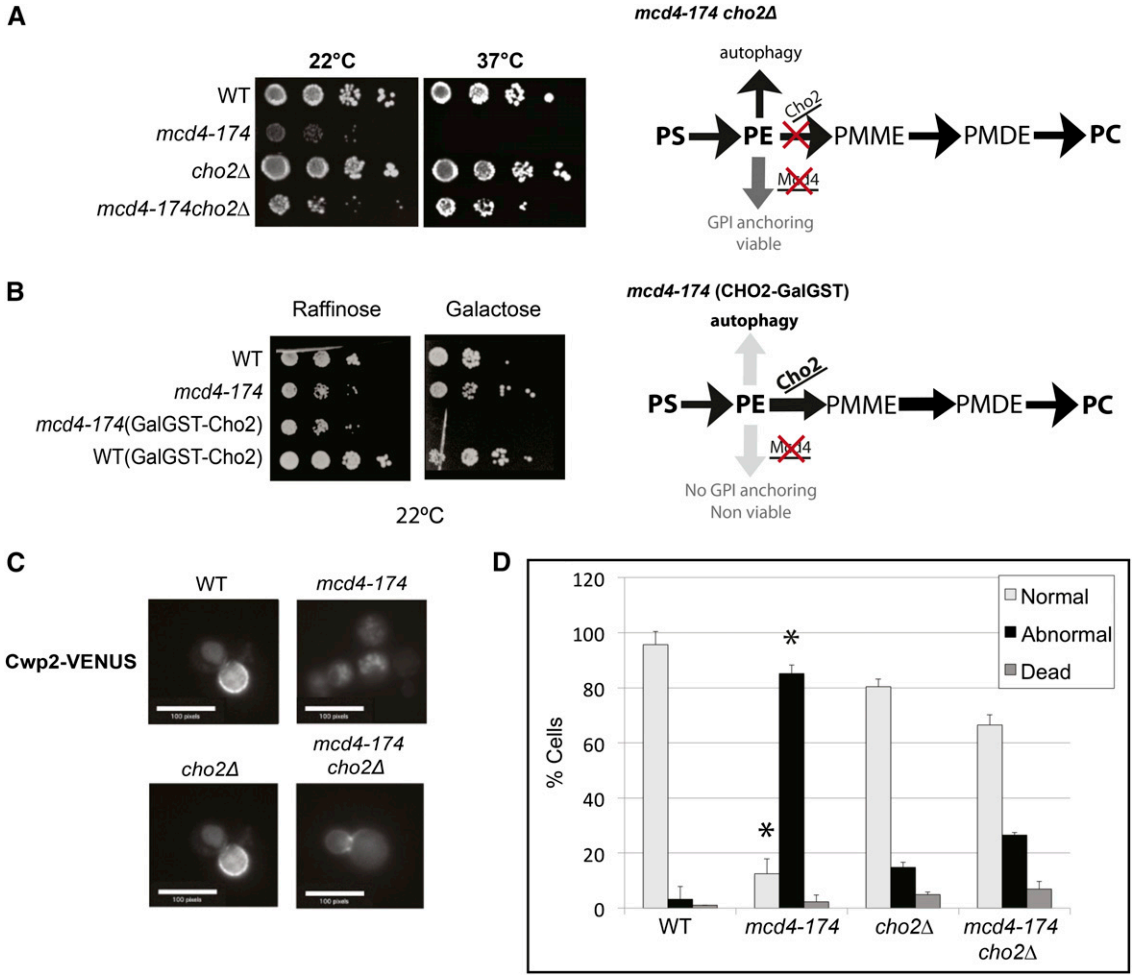

Figure 3 Alterations to the phospholipid synthesis pathway can rescue or exacerbate defects in an *mcd4-174* strain. (A) Dilution spotting of WT and mutant yeast cells grown at permissive (22°) and nonpermissive (37°) temperatures in rich medium. Deletion of *CHO2*, a component of the phospholipid synthesis pathway, can partially rescue lethality of *mcd4-174* at restrictive temperature. In a *cho2Δ* mutant, PC formation through the *de novo* pathway is reduced, and the flux of PE is pushed toward GPI anchoring, causing a partial rescue. (B) Dilution spotting of WT and mutant yeast cells grown at permissive (22°) temperature in medium supplemented with either raffinose or galactose, in which Cho2 overexpression is galactose induced. On Cho2 overexpression (galactose), the flux of PE is pushed toward PC formation, further impairing the residual activity of *mcd4-174* at permissive temperature (22°). (C) The localization of GPI-anchored protein Cwp2-VENUS was examined by microscopic analysis in WT and the indicated mutant strains as per Figure 2C. Localization of Cwp2-VENUS is partially restored in a *mcd4-174 cho2Δ* mutant. (D) Graph is quantitation of the images in (C) carried out as described in Figure 2D.

Cells with decreased Mcd4 activity exhibit reduced PE levels

We have discovered that cells with reduced Mcd4 activity also exhibit decreased levels of PE at 37°, and this defect is at least partially responsible for their slow-growth defect. Why PE levels are reduced in this mutant is less clear. Mcd4 catalyzes the first ethanolamine phosphate transferase reaction in the GPI synthesis pathway and uses PE as a precursor to synthesize the membrane anchor. The mutation causing ts growth of *mcd4-174* cells is located within a motif that is conserved in phosphodiesterases and pyrophosphatases and changes glycine 227 to a glutamic acid residue. A simple explanation for the lower PE levels is that rather than transferring the ethanolamine phosphate from PE to the GPI precursor, the mutant enzyme simply hydrolyses the PE without efficiently completing the transfer. Previous studies have shown an increase in ethanolamine phosphate in a *mcd4-174* mutant (Storey *et al.* 2001), providing a precedent for this hypothesis. Alternatively, WT Mcd4 also may be involved in regulating PE levels through a different mechanism. PS levels are lower in all *mcd4-174* single and double mutants at restrictive temperature (Table S2) and may limit the amount of precursor available for PE synthesis. Mcd4 also might regulate the activity of the PC synthesis and/or degradation pathway. Finally, the failure to export GPI-anchored proteins may induce ER-phagy and thus cause vacuolar digestion of membranes and large-scale hydrolysis of PE. Irrespective of the underlying molecular explanation, it is clear that addition of exogenous ethanolamine or an increase in intracellular PE levels by reducing the flux of this lipid through autophagy or PC synthesis suppresses most, if not all, phenotypes observed with the *mcd4-174* mutant. It is unlikely that Mcd4 plays a direct role in

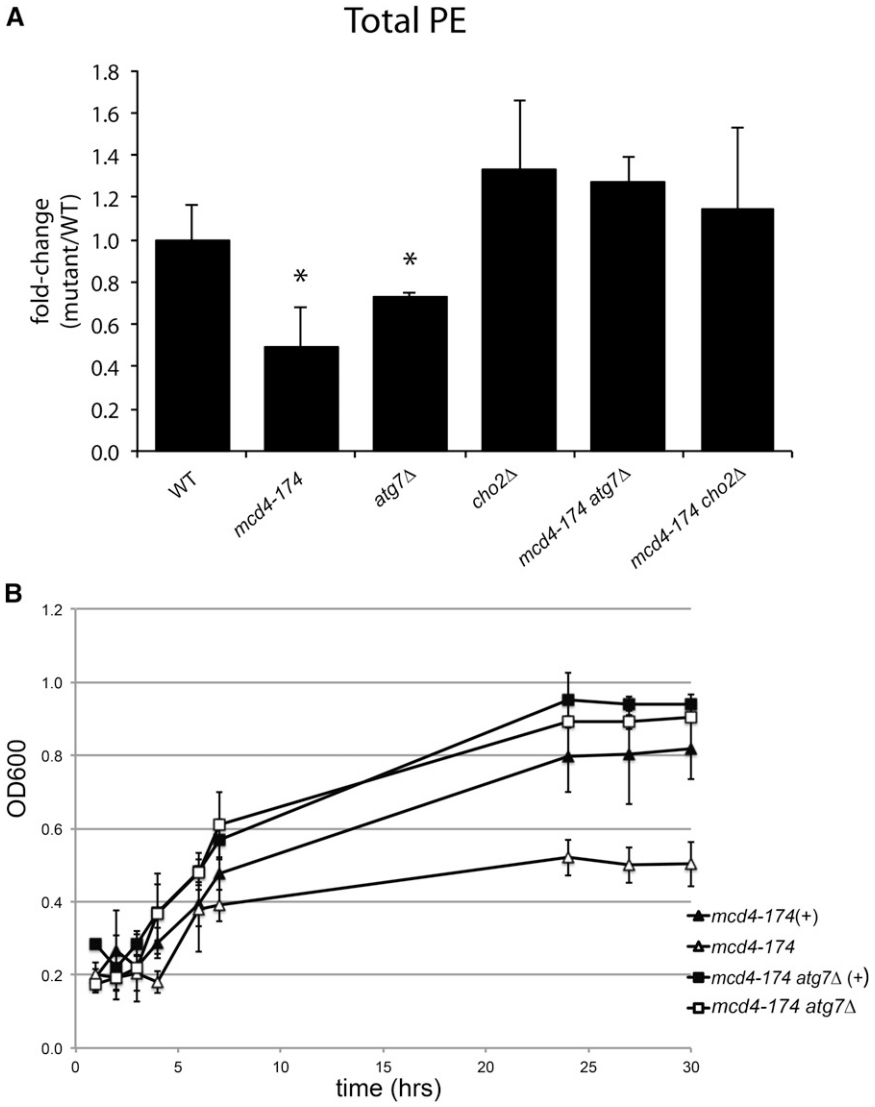

Figure 4 Loss of autophagy restores PE levels in *mcd4-174* grown at restrictive temperature. (A) Lipid analysis shows that total PE levels after growth at 37° were reduced in *mcd4-174* strains and increased in *mcd4-174 atg7*Δ and *mcd4-174 cho2*Δ. The total amount of PE was calculated as the sum of all PE species. Data are average and SD of independent biological replicates ($n = 3$), shown in the "Summary" of Table S2. *$P < 0.05$, *t*-test as compared with WT. (B) Growth curves of mutant yeast strains measuring OD_{600} change over time. Addition of 5 mM ethanolamine to the medium can partially rescue the growth of *mcd4-174* cells at restrictive temperature. The growth of WT (not shown) or *mcd4-174 atg7*Δ cells was unaffected by the addition of ethanolamine. Data are average and SD of independent biological replicates ($n = 3$).

autophagy. The autophagy defects observed in the *mcd4-174* mutant are probably caused indirectly by the reduction of one or more particular pools of PE or the massively proliferated and possibly disturbed Golgi and ER compartments.

Regulation of PE synthesis and flux in major PE-consuming pathways

Our data suggest that the GPI anchor biosynthesis competes with autophagy and PC biosynthesis for a common PE pool. Under nutrient-rich conditions, PE production in WT cells is mainly directed to the synthesis of GPI anchors and PC production. This flux may change under starvation conditions because a substantial amount of PE is required for autophagosome formation during autophagy and thus is diverted away from the GPI anchor biosynthesis pathway. PE levels are reduced in the *mcd4-174* cells, which renders them sensitive to Cho2 overexpression or deletion of *PSD2 or ECT1*. Conversely, the viability of *mcd4-174* but not *mcd4Δ* cells is rescued by deletion of *CHO2* or essential autophagy genes. We thus speculate that under starvation conditions, the conversion from PE to PC may be temporally inhibited to increase the availability of PE for autophagy while maintaining a basal level of GPI anchor synthesis to strengthen the cell wall. The mechanism of this inhibition is unclear at present but may include regulation of the activity of Cho1 or Cho2 by post-translational modifications such as phosphorylation or allosteric binding of metabolites. Alternatively, direct binding to Atg8 could alter their enzymatic activity or localization, and indeed, a potential conserved LC3-interacting region (LIR) is present in Cho2. Clearly, further work is required to elucidate the mechanisms of how PE flux through the major PE-consuming pathways is regulated and balanced to cope with the changing cellular needs.

Acknowledgments

We thank Charlie Boone for the ts yeast library and Dennis Voelker for the *mcd4-P301L* strain. We are grateful to Ingrid

Stoffel-Studer, Janny Tilma, and Isabelle Riezman for technical support, Fabrice David for help with analysis of the mass spectrometry data, Serge Pelet for the Goldeneye software, and Alicia Smith for critical reading of the manuscript. M.P. is supported by the European Research Council (ERC), the Swiss National Science Foundation (SNSF), and ETH Zürich; F.R. by the ALW Open Program (821.02.017 and 822.02.014), the DFG-NWO cooperation (DN82-303), and ZonMW-VIDI (917.76.329) and ZonMW-VICI (016.130.606) grants; and H.R. by SystemsX.ch (LipidX.ch, evaluated by the SNSF) and the SNSF.

Literature Cited

Behrends, C., M. E. Sowa, S. P. Gygi, and J. W. Harper, 2010 Network organization of the human autophagy system. Nature 466: 68–76.

Birner, R., M. Burgermeister, R. Schneiter, and G. Daum, 2001 Roles of phosphatidylethanolamine and of its several biosynthetic pathways in Saccharomyces cerevisiae. Mol. Biol. Cell 12: 997–1007.

Blamowska, M., M. Sichting, K. Mapa, D. Mokranjac, W. Neupert *et al.*, 2010 ATPase domain and interdomain linker play a key role in aggregation of mitochondrial Hsp70 chaperone Ssc1. J. Biol. Chem. 285: 4423–4431.

Canivenc-Gansel, E., I. Imhof, F. Reggiori, P. Burda, A. Conzelmann *et al.*, 1998 GPI anchor biosynthesis in yeast: phosphoethanolamine is attached to the α1,4-linked mannose of the complete precursor glycophospholipid. Glycobiology 8: 761–770.

Carman, G. M., and G. S. Han, 2011 Regulation of phospholipid synthesis in the yeast Saccharomyces cerevisiae. Annu. Rev. Biochem. 80: 859–883.

Castillon, G. A., R. Watanabe, M. Taylor, T. M. Schwabe, and H. Riezman, 2009 Concentration of GPI-anchored proteins upon ER exit in yeast. Traffic 10: 186–200.

Cheng, J., T. S. Park, A. S. Fischl, and X. S. Ye, 2001 Cell cycle progression and cell polarity require sphingolipid biosynthesis in Aspergillus nidulans. Mol. Cell. Biol. 21: 6198–6209.

Conzelmann, A., H. Riezman, C. Desponds, and C. Bron, 1988 A major 125-kd membrane glycoprotein of Saccharomyces cerevisiae is attached to the lipid bilayer through an inositol-containing phospholipid. EMBO J. 7: 2233–2240.

Gaynor, E. C., G. Mondesert, S. J. Grimme, S. I. Reed, P. Orlean *et al.*, 1999 MCD4 encodes a conserved endoplasmic reticulum membrane protein essential for glycosylphosphatidylinositol anchor synthesis in yeast. Mol. Biol. Cell 10: 627–648.

Griffith, J., M. Mari, A. De Maziere, and F. Reggiori, 2008 A cryosectioning procedure for the ultrastructural analysis and the immunogold labelling of yeast Saccharomyces cerevisiae. Traffic 9: 1060–1072.

Guan, X. L., I. Riezman, M. R. Wenk, and H. Riezman, 2010 Yeast lipid analysis and quantification by mass spectrometry. Methods Enzymol. 470: 369–391.

Harding, T. M., K. A. Morano, S. V. Scott, and D. J. Klionsky, 1995 Isolation and characterization of yeast mutants in the cytoplasm to vacuole protein targeting pathway. J. Cell Biol. 131: 591–602.

He, H., Y. Dang, F. Dai, Z. Guo, J. Wu *et al.*, 2003 Post-translational modifications of three members of the human MAP1LC3 family and detection of a novel type of modification for MAP1LC3B. J. Biol. Chem. 278: 29278–29287.

Henry, S. A., S. D. Kohlwein, and G. M. Carman, 2012 Metabolism and regulation of glycerolipids in the yeast *Saccharomyces cerevisiae*. Genetics 190: 317–349.

Hong, B., J. S. Brockenbrough, P. Wu, and J. P. Aris, 1997 Nop2p is required for pre-rRNA processing and 60S ribosome subunit synthesis in yeast. Mol. Cell. Biol. 17: 378–388.

Hong, Y., Y. Maeda, R. Watanabe, K. Ohishi, M. Mishkind *et al.*, 1999 Pig-n, a mammalian homologue of yeast Mcd4p, is involved in transferring phosphoethanolamine to the first mannose of the glycosylphosphatidylinositol. J. Biol. Chem. 274: 35099–35106.

Hutchins, M. U., and D. J. Klionsky, 2001 Vacuolar localization of oligomeric α-mannosidase requires the cytoplasm to vacuole targeting and autophagy pathway components in Saccharomyces cerevisiae. J. Biol. Chem. 276: 20491–20498.

Kim, J., W. P. Huang, and D. J. Klionsky, 2001 Membrane recruitment of Aut7p in the autophagy and cytoplasm to vacuole targeting pathways requires Aut1p, Aut2p, and the autophagy conjugation complex. J. Cell Biol. 152: 51–64.

Li, Z., F. J. Vizeacoumar, S. Bahr, J. Li, J. Warringer *et al.*, 2011 Systematic exploration of essential yeast gene function with temperature-sensitive mutants. Nat. Biotechnol. 29: 361–367.

McGraw, P., and S. A. Henry, 1989 Mutations in the *Saccharomyces cerevisiae opi3* gene: effects on phospholipid methylation, growth and cross-pathway regulation of inositol synthesis. Genetics 122: 317–330.

McMaster, C. R., and R. M. Bell, 1994 Phosphatidylcholine biosynthesis via the CDP-choline pathway in Saccharomyces cerevisiae: multiple mechanisms of regulation. J. Biol. Chem. 269: 14776–14783.

Meiling-Wesse, K., H. Barth, C. Voss, E. L. Eskelinen, U. D. Epple *et al.*, 2004 Atg21 is required for effective recruitment of Atg8 to the preautophagosomal structure during the Cvt pathway. J. Biol. Chem. 279: 37741–37750.

Motley, A. M., J. M. Nuttall, and E. H. Hettema, 2012 Atg36: the Saccharomyces cerevisiae receptor for pexophagy. Autophagy 8: 1680–1681.

Noda, N. N., Y. Ohsumi, and F. Inagaki, 2010 Atg8-family interacting motif crucial for selective autophagy. FEBS Lett. 584: 1379–1385.

Papinski, D., M. Schuschnig, W. Reiter, L. Wilhelm, C. A. Barnes *et al.*, 2014 Early steps in autophagy depend on direct phosphorylation of Atg9 by the Atg1 kinase. Mol. Cell 53: 471–483.

Santos, A., I. Riezman, A. Aguilera-Romero, F. David, M. Piccolis *et al.*, 2014 Systematic lipidomic analysis of yeast protein kinase and phosphatase mutants reveals novel insights into regulation of lipid homeostasis. Mol. Biol. Cell. (in press).

Storey, M. K., W. I. Wu, and D. R. Voelker, 2001 A genetic screen for ethanolamine auxotrophs in Saccharomyces cerevisiae identifies a novel mutation in Mcd4p, a protein implicated in glycosylphosphatidylinositol anchor synthesis. Biochim. Biophys. Acta 1532: 234–247.

Sutterlin, C., A. Horvath, P. Gerold, R. T. Schwarz, Y. Wang *et al.*, 1997 Identification of a species-specific inhibitor of glycosylphosphatidylinositol synthesis. EMBO J. 16: 6374–6383.

Suzuki, K., Y. Kamada, and Y. Ohsumi, 2002 Studies of cargo delivery to the vacuole mediated by autophagosomes in Saccharomyces cerevisiae. Dev. Cell 3: 815–824.

Suzuki, K., C. Kondo, M. Morimoto, and Y. Ohsumi, 2010 Selective transport of alpha-mannosidase by autophagic pathways: identification of a novel receptor, Atg34p. J. Biol. Chem. 285: 30019–30025.

Suzuki, K., Y. Kubota, T. Sekito, and Y. Ohsumi, 2007 Hierarchy of Atg proteins in pre-autophagosomal structure organization. Genes to Cells 12: 209–218.

Toh-e, A., and T. Oguchi, 2002 Genetic characterization of genes encoding enzymes catalyzing addition of phospho-ethanolamine to the glycosylphosphatidylinositol anchor in Saccharomyces cerevisiae. Genes Genet. Syst. 77: 309–322.

Tong, A. H., M. Evangelista, A. B. Parsons, H. Xu, G. D. Bader *et al.*, 2001 Systematic genetic analysis with ordered arrays of yeast deletion mutants. Science 294: 2364–2368.

Xie, Z., U. Nair, and D. J. Klionsky, 2008 Atg8 controls phagophore expansion during autophagosome formation. Mol. Biol. Cell 19: 3290–3298.

Xin, Y., L. Yu, Z. Chen, L. Zheng, Q. Fu *et al.*, 2001 Cloning, expression patterns, and chromosome localization of three human and two mouse homologues of GABA(A) receptor-associated protein. Genomics 74: 408–413.

Yuga, M., K. Gomi, D. J. Klionsky, and T. Shintani, 2011 Aspartyl aminopeptidase is imported from the cytoplasm to the vacuole by selective autophagy in Saccharomyces cerevisiae. J. Biol. Chem. 286: 13704–13713.

Zhu, H., M. Bilgin, R. Bangham, D. Hall, A. Casamayor *et al.*, 2001 Global analysis of protein activities using proteome chips. Science 293: 2101–2105.

Zhu, Y., C. Vionnet, and A. Conzelmann, 2006 Ethanolaminephosphate side chain added to glycosylphosphatidylinositol (GPI) anchor by mcd4p is required for ceramide remodeling and forward transport of GPI proteins from endoplasmic reticulum to Golgi. J. Biol. Chem. 281: 19830–19839.

Communicating editor: D. J. Lew

GENETICS

Supporting Information
http://www.genetics.org/lookup/suppl/doi:10.1534/genetics.114.169797/-/DC1

Autophagy Competes for a Common Phosphatidylethanolamine Pool with Major Cellular PE-Consuming Pathways in *Saccharomyces cerevisiae*

Caroline Wilson-Zbinden, Aline Xavier da Silveira dos Santos, Ingrid Stoffel-Studer, Aniek van der Vaart, Kay Hofmann, Fulvio Reggiori, Howard Riezman, Claudine Kraft, and Matthias Peter

DOI: 10.1534/genetics.114.169797

File S1

Strains and Plasmids

Yeast strains used in this study

Name	Genotype	Background	Source
BY4741	Mat a; *his3Δ1; leu2Δ0; met15Δ0; ura3Δ0*	S288C	Euroscarf
BY7220	*can1*::STE2pr-Sp_*his5 ura3*::NatR *lyp1Δ cyh2 his3Δ leu2Δ met1Δ0*; yMSo261	S288C	Boone lab
BY7092	*can1*::STE2pr-Sp_*his5 ura3*::NatR *lyp1Δ cyh2 his3Δ leu2Δ met1Δ0*; yMSo261; *atg1Δ::*natMX4	S288C	Boone lab
yCW188	BY4741; *mcd4-174*:kanMX4	S288C	Boone lab
yCW95	BY4741; *gpi8-ts*:kanMX4	S288C	Boone lab
yCW10	BY4741; *atg7Δ::*natMX4	S288C	This study
yCW372	BY4741; *mcd4-174*:kanMX4;*atg7Δ::*natMX4	S288C	This study
yCW179	BY4741; *atg14Δ::*natMX4	S288C	This study
yCW177	BY4741; *mcd4-174::*kanMX4; *atg14Δ::*kanMX4	S288C	This study
yCW261	BY4741; *atg21Δ::*natMX4	S288C	This study
yCW375	BY4741; *mcd4-174*::kanMX4; *atg21Δ::*natMX4	S288C	This study
yCK406	BY4741; *atg1Δ::*natMX4	S288C	Claudine Kraft
yCW320	BY4741; *mcd4Δ::*kanMX4; *atg1Δ::*natMX4	S288C	This study
yCW96	BY4741; *gpi2-1*::kanMX4	S288C	This study
yCW118	BY4741; *gpi2-1*::kanMX4; *atg7Δ::*natMX4	S288C	This study
yCW92	BY4741; *gpi13-5::*kanMX4	S288C	This study
yCW117	BY4741; *gpi13-5*::kanMX4; *atg7Δ::*natMX4	S288C	This study
yCK68	BY4741; *pep4Δ::*natMX4	S288C	Claudine Kraft

yCW41	BY4741; *mcd4-174*::kanMX4; *pep4Δ::*natMX4	S288C	This study
yCW475	BY4741; *atg7Δ::*kanMX4; *pep4Δ::*natMX4	S288C	This study
yCW42	BY4741; *mcd4-174::*kanMX4; *pep4Δ::*natMX4; *atg7Δ::*natMX4	S288C	This study
yCW361	BY4741; *cho2Δ::*natMX4	S288C	This study
yCW364	BY4741; *mcd4-174*::kanMX4; *cho2Δ::*kanMX4	S288C	This study
RYY52	MATα *trp1, lys2, ura3, leu2, his3, suc2, psd1Δ-1*::TRP1	S288C	Voelker Lab
MKY3	MATα *trp1, lys2, ura3, leu2, his3, psd1Δ-1*::TRP1, *mcd4-P301L*, etn−ts	S288C	Voelker Lab

Plasmids used in this study

Name	**Characteristics**	**Source**
pCW58	p5472; MCD4	Thermo Scientific
pCW59	p5472; ATG7	Thermo Scientific
pCW73	p5472; ATG14	Thermo Scientific
pCW74	p5472; ATG21	Thermo Scientific
pCK15	pRS316; GFP-ATG8	Claudine Kraft
pCW75	p416; CWP2-VENUS	Riezman lab
pCW76	GAL1/10; GST-CHO2	Thermo Scientific

Table S1 Synthetic-lethality and suppression analysis of *ts*-strains with *ATG1* and other autophagy genes. The isogenic temperature-sensitive strain collection (LI *et al.* 2011) was crossed with cells deleted for *ATG1*, and synthetic-lethality (A) or suppression (B) was determined by SGA analysis at 30° or 37°, respectively. The phenotype of the double mutants was verified by tetrad analysis, and the strength of the suppression or slow growth defect was scored based on colony size. +++: strong interaction; ++: medium interaction; +: weak interaction. The genetic interaction was also analyzed by crossing the strains to *atg7Δ* cells to determine whether the phenotype was specific for *ATG1* or shared with other autophagy mutants.

A

Allele Name	Systematic Name	Restrictive Temperature	Strength of Phenotype	*atg1Δ* Specific
gpi8-ts	YDR331w	35	++	Y
nop2-4	YNL061w	30-35	++	Y
orc3-70	YLL004w	30	++	Y
ssc1-2	YJR045c	30	++	Y
ycg1-2	YDR325w	30-35	++	Y

B

Allele Name	Systematic Name	Restrictive Temperature	Strength of Phenotype	*atg1Δ* Specific
cmd1-3	YBR109c	37	++	Y
hyp2-8	YEL034w	35	+++	N
mcd4-174	YKL165c	37	+++	N
okp1-5	YGR179c	35	++	Y
sec17-1	YBL050w	37	++	Y

Table S2 Lipid analysis data. Lipid analysis shows that total PE levels after growth at 37° were reduced in *mcd4-174* strains, and increased in *mcd4-174 atg7*Δ and *mcd4-174 cho2*Δ. Data are average and standard deviation of independent biological replicates (n=3), normalized to wild-type controls (units= fold-change (mutant/WT)). (*) $p<0.05$, t-test as compared to WT.

Available for download as an Excel file at

http://www.genetics.org/lookup/suppl/doi:10.1534/genetics.114.169797/-/DC1

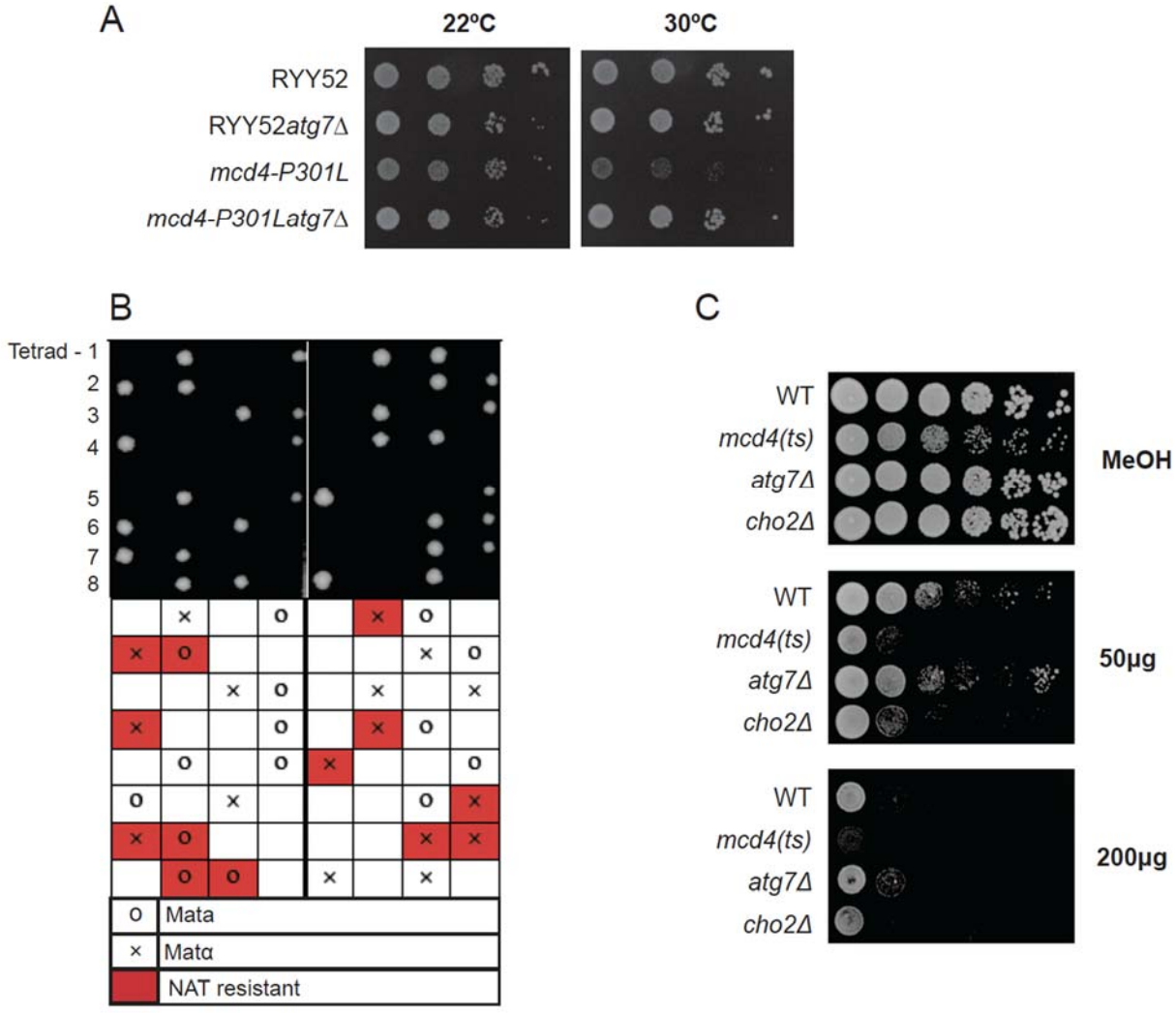

Figure S1 Deletion of general autophagy restores growth of mcd4-P301L cells but cannot rescue lethality of *mcd4*Δ. (a) Dilution spotting of wild-type (RYY52) and mutant yeast cells (*mcd4-P301L*) grown at permissive (22°) and non-permissive (30°) temperatures in synthetic complete media. Deletion of *ATG7* rescues lethality of mutant cells at restrictive temperature. (b) Tetrad analysis of diploid cells heterozygous for *mcd4Δ::KAN* and *atg7Δ::NAT*. Each tetrad displays only two viable spores neither of which corresponds to the double deletion strain. (c) Wild-type (WT) and the indicated mutant cells were spotted in 10-fold dilutions on plates containing the 50 or 200 µg of the Mcd4-inhibitor YW3548 or methanol (MeOH) as the solvent control. Note that *atg7Δ* or *cho2Δ* cells show the same sensitivity to the drug as wild-type controls.

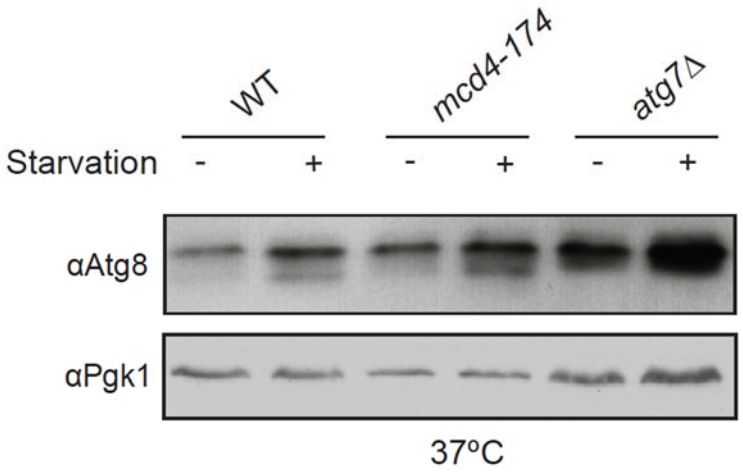

Figure S2 The general autophagy defect of *mcd4-174* cells is not caused by reduced Atg8-PE levels. Western blot analysis comparing the levels of lipidated Atg8-PE in wild-type (WT), *mcd4-174* or *atg7Δ* cells. Where indicated (+), autophagy was induced by growing the cells for three hours in starvation medium at 37°. Note that reduced Mcd4-function does not significantly alter lipidation of Atg8, implying that the observed autophagy defect may results from defects downstream of Atg8 activation.

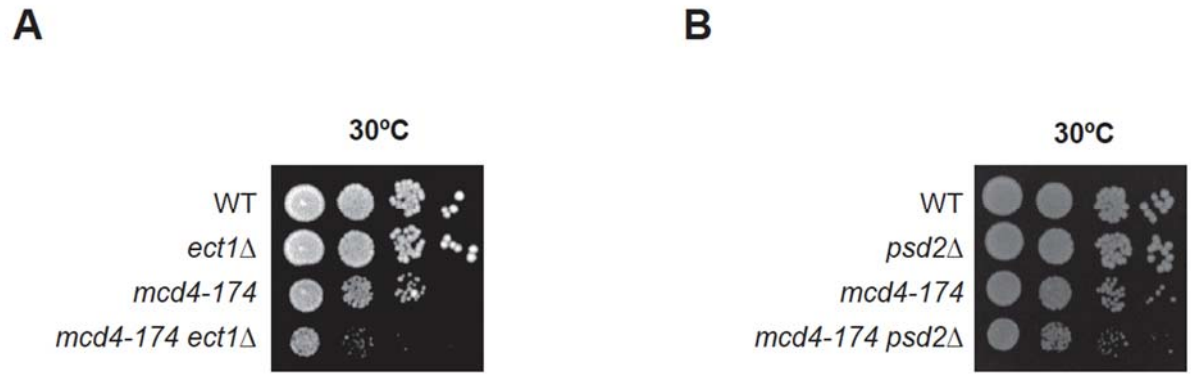

Figure S3 Alterations to the phospholipid synthesis pathway exacerbate the growth defects of *mcd4-174* cells at semi-permissive temperature. (a and b) Dilution spottings of *mcd4-174* cells crossed to strains lacking either *ECT1* (a) or *PSD2* (b) encoding enzymes involved in the CDP-ethanolamine pathway or the conversion of PS to PE in vacuolar membranes, respectively. Plates were photographed after incubation for 3 days at semi-permissive temperature (30°).